

## Optimization of hole generation in Ti/CFRP stacks

Y N Ivanov, A E Pashkov, N S Chashhin

Irkutsk National Research Technical University, 83 Lermontov Street, Irkutsk, 664074, Russia

Tomsk Polytechnic University, 30, Lenina Av., Tomsk, 634050, Russia

E-mail: [iv\\_yuriy@istu.edu](mailto:iv_yuriy@istu.edu)

**Abstract.** The article aims to describe methods for improving the surface quality and hole accuracy in Ti/CFRP stacks by optimizing cutting methods and drill geometry. The research is based on the fundamentals of machine building, theory of probability, mathematical statistics, and experiment planning and manufacturing process optimization theories. Statistical processing of experiment data was carried out by means of Statistica 6 and Microsoft Excel 2010. Surface geometry in Ti stacks was analyzed using a Taylor Hobson Form Talysurf i200 Series Profilometer, and in CFRP stacks - using a Bruker ContourGT-K1 Optical Microscope. Hole shapes and sizes were analyzed using a Carl Zeiss CONTURA G2 Measuring machine, temperatures in cutting zones were recorded with a FLIR SC7000 Series Infrared Camera. Models of multivariate analysis of variance were developed. They show effects of drilling modes on surface quality and accuracy of holes in Ti/CFRP stacks. The task of multicriteria drilling process optimization was solved. Optimal cutting technologies which improve performance were developed. Methods for assessing thermal tool and material expansion effects on the accuracy of holes in Ti/CFRP/Ti stacks were developed.

### 1. Introduction

New generation aircrafts incorporate tons of CFRP in their structures. One of the main aircraft construction tasks is to ensure durable connection of CFRP and metal parts. Those combinations are referred to as hybrid stacks. The article describes technology development results for the hole generation in hybrid stacks of MS-21 wing center section junctures. The hole diameter is 14 mm with 9 grade of accuracy, the total stack thickness is 35-45 mm. The stack consists of two Titanium layers and one middle CFRP layer. The target surface roughness in Titanium is Ra 1.6.

Drilling of Ti/CFRP stacks is a hard process task. The researches [1-2] identified a significant difference of the cutting mechanism with application of the Ti/CFRP edge tool. When machining titanium, chip is generated due to plastic deformation of the cutting face [3]. Machining CFRP is different due to the anisotropy of CFRP properties [1]. The main factor decreasing performance of machining CFRP is an abrasive nature of the filler causing a fast tool wear and temperature rise in the cutting zone which destroy a plastic binder. To minimize CFRP drawbacks, it is necessary to increase cutting and feed rates. However, for Ti/CFRP stacks, this requirement generates doubts due to significant heat radiation [4-6]. Owing to the proneness to water absorption, it is not allowed to use liquids for cooling CFRP stacks [7]. Only a minimum quantity of lubricant (MQL) and compressed air feeding can be used [8].

For the hole generation in CFRP/Ti stacks, hard metal tools with cutting parts with/without low-



wear coating, PCD tools with cutting parts and other special tools can be used. Suppliers of those tools are Precor, Kennametal (USA), Sandvik Coromant, SECO (Sweden), Mapal (Germany) et al. As a rule, the drilling does not ensure 10-11 grade of accuracy. Accuracy can be increased by hole trueing and reaming in order to increase a hole generation speed rate.

To improve the surface quality and hole accuracy in CFRP/Ti stacks, it is necessary to study thermal effects on hole shapes, and optimize the drilling process with regard to target parameters of surface quality, accuracy and performance.

## 2. Variation in the hole shape due to the thermal expansion

Let us calculate the longitudinal section profile deviation due to thermal factors taking into account that Titanium and CFRP have different linear expansion coefficients and local temperatures during the cutting process. Based on the average temperature values, let us determine the thermal deformations using high accuracy imaging IR equipment.

During the cutting, the tool edge interacting with the material heats up and increases its radial length (see Figure 1a). Increase in a tool diameter  $\Delta I$  is a difference between final and initial temperatures in the area of the main edge and a linear expansion coefficient for the tool material.

Part heating is less intensive as the rotating tool takes one and the same radial position in time intervals in which heat dissipates. Thermal deformation of the material  $\Delta M$  (see Figure 1b) is a difference between final and initial temperatures of the material in the cutting zone and a linear expansion coefficient.

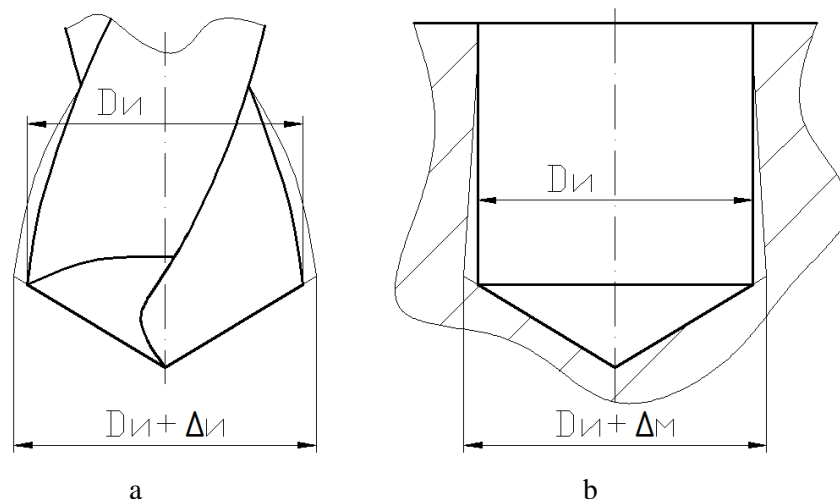


**Figure 1.** Deformations of the drill (a); of the machined material (b) during the drilling.

Thermal tool deformation increases a hole diameter, while material deformation decreases it as the thermal load reduction makes the material diminish in volume. The resultant effect on the diameter in the radial hole section  $i$  can be presented as:

$$\Delta i = \Delta I - \Delta M \quad (1)$$

The longitudinal hole section profile deviation caused by thermal deformations is a half difference between maximum and minimum values  $\Delta_i$  calculated for all radial hole sections. At hole depth  $h$ , the longitudinal section profile deviation value can be expressed as:

$$\Delta = \frac{\max_{0 \leq i \leq h} \Delta_i - \min_{0 \leq i \leq h} \Delta_i}{2} \quad (2)$$

The maximum value  $\Delta_i$  can be observed at the moment when the tool heats up, but its expansion is not compensated by the material expansion. A section corresponding to the beginning of the drilling of the first titanium layer meets this requirement. At this moment, tool edges heat up, and the material began heating up. The minimum value  $\Delta_i$  can be observed at lower cutting temperatures when the tool expansion is compensated by the expansion caused by the material heating. It occurs in the section corresponding to the cutting temperature in the composite material. After the holes in titanium stacks

have been drilled, the temperature of drill edges decreases, and the work material heats up in the cutting zone to steady-state temperature values.

Thus, for Ti/CFRP/Ti stacks, the longitudinal section profile deviation can be written as:

$$\Delta = \frac{\Delta_{Ti1(enter)} - \Delta_{CFRP(ss)}}{2} \quad (3)$$

where  $\Delta_{Ti1(enter)}$  – effects of thermal deformations in the first titanium layer,  $\Delta_{CFRP(ss)}$  effects of thermal deformations in the CFRP layer at steady-state cutting temperature values.

### 3. Effects of drilling parameters on hole quality

According to the analysis of research data, hole accuracy is influenced by process parameters – cutting speed and feed rates (key factors) and some additional parameters (lubrication, cooling, chip removal) [9-12]. Due to a complex nature of the effects of drilling parameters on hole accuracy and quality, regression analysis and experiment planning methods were used to reveal relations between input and output parameters [2], [13-14]. Taking into account that the tool life is within the range of 30-50 holes [15], it is necessary to take measures to remove the impact of “the state of the cutting tool” on key effects assessment. To this end, let us divide the experiment into separate blocks where the tool state is considered unchangeable. Let us express the factor “the state of the cutting tool” in the cutting length of the tool and use a three-level factorial plan 3(3-1) with two key factors and one block factor. The number of experiments is N=9, the number of repetitions is n=3. The plan is implemented using Statistica 6. The order of experiments is randomized in order to prevent result corruption due to bias errors.

Many relations can be presented as polynomial equations [16]:

$$Y = cv^{\alpha}s^{\beta}t^{\gamma}, \quad (4)$$

where v – cutting speed rate; s – feed rate; t – cutting depth; c,  $\alpha$ ,  $\beta$ ,  $\gamma$  – constant coefficients. The cutting depth is a constant value, so it is eliminated from the equation. Cutting length l is introduced in the equation which can be written as:

$$Y = cv^{\alpha}s^{\beta}l^{\gamma}. \quad (5)$$

By taking the logarithm, the equation (7) can be linearized and written as:

$$\hat{y} = b_0 + b_1x_1 + b_2x_2 + b_3x_3, \quad (6)$$

where  $\hat{y} = \ln Y$ ;  $x_1, x_2, x_3$  – coded factor values v, s, l [27].

$$x_i = \frac{2(\ln \tilde{x}_{iB} - \ln \tilde{x}_{iH})}{\ln \tilde{x}_{iB} - \ln \tilde{x}_{iH}} + 1, \quad (7)$$

where  $\tilde{x}_i$  – natural value;  $\tilde{x}_{iB}, \tilde{x}_{iH}$  – natural values of the upper and lower levels.

To assess equation coefficients, experiment results can be written as:

$$\hat{y} = b_0 + b_1x_1 + b_2x_2 + b_3x_3 + b_{12}x_1x_2 + b_{11}x_1^2 + b_{22}x_2^2 + b_{33}x_3^2 \quad (8)$$

Cutting parameter optimization involves searching for an extremum of the criterion of one type or another or their combination. Statistica 6 implements the method for determining an optimum based on the models developed as a result of the multivariate analysis of variances. Based on the optimization methods, let us determine the best hole generation parameters which meet target quality and accuracy requirements.

### 4. Experimental methods and conditions

Experiments were carried out using a pneumatic automatic feed drill Atlas Copco PFD-1500 which allows discrete variations in feed and spindle rotation rates. Lubrication and cooling of the cutting zone were carried out with Accu-Lube LB-5000 MQL. Lubricant consumption was 0.3 g/min. Three-layer stacks with structures similar to a MS-21 outer wing and center wing juncture were used. The hybrid stack consists of two titanium (VT6 OST 1.90218-76) layers and one middle CFRP layer (a PRISM EP2400 RS binder; an IMS 24K carbonic band with a monolayer thickness of 0.19 mm. The layup pattern is symmetric, balanced; layer directions are 0°, 90°, +45°, -45°). Stack sheets were

joined with bolts. The stack was not taken to layers to eliminate prediction errors. As a key cutting tool, a Sandvik Coromant CoroDrill 86PT Series PCD drill was used.

Variable process parameters were cutting speed and feed rates. The additional parameter (block factor) was the state of the cutting tool determined as a cutting length by formula:

$$l_k = \sum_{i=1}^k \frac{\pi dh}{s_i}, \quad (9)$$

where  $d$  – tool diameter,  $h$  – hybrid stack thickness,  $s_i$  – feed in the  $i$ -th test of the experiment,  $k$  – number of the test for which the cumulative cutting length should be determined.

At the first stage, the samples were being kept in a temperature-controlled room at a temperature of 20 °C within 24 hours. Diameter sizes and circularity deviations were measured using a Carl Zeiss CONTURA G2 Series measuring machine. The measurements were carried out in different radial sections by means of circular scanning of points. Then longitudinal section profile deviation values were determined. Circularity deviations were measured in average sections of each stack layer.

Roughness parameters  $R_a$  and  $R_z$  in titanium samples were measured using a Taylor Hobson Form Talysurf i200 Series profilometer with a diamond-ended probe of 2 micrometer in a radius. Four hole elements were measured at straight angles. To analyze profilographs, a Gaussian filter was used. A bandwidth is 300:1 (by ISO), a sampling length is 0.8 mm. CFRP roughness was controlled using a Bruker ContourGT-K1 Series profilometer. Rectangular scanning zones of 1.1x4 mm in size were selected by four hole elements. As a result, the authors had the CFRP surface topography (see Figure 2) with calculated  $R_a$  and  $R_z$ . An average value was calculated by four stated roughness values.

To determine thermal effects on the hole accuracy, a visual access to the drilling zone was created using a FLIR SC7000 Series Infrared Camera installed at a distance of 700 mm from the cutting zone at the level of a drill axis in a horizontal plane, and at an angle of 40 degrees to the sample surface (see Figure 3a). Canted shooting allows simultaneous recording of tool edge and sample surface material temperatures (see Figure 3b).

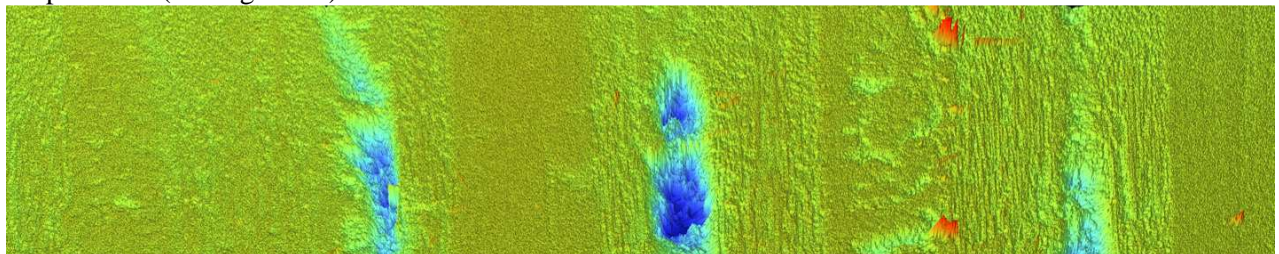


**Figure 2.** CFRP surface topography

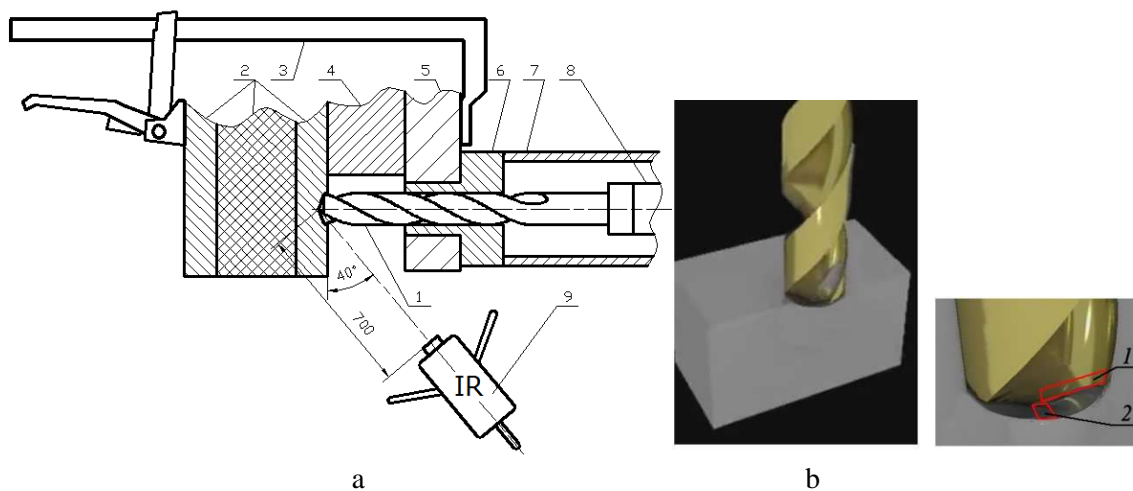


**Figure 3.** Temperature recording in the cutting zone (a): 1 – drill; 2 – sample; 3 – clamp; 4 – support; 5 – conductor; 6 – AFD bush; 7 – AFD head; 8 – AFD spindle; 9 – infrared camera; cutting temperature recording zones for (b): 1 – tool; 2 – material

## 5. Experimental results

Standard results of drilled hole shape measurements are shown in Figure 4a.

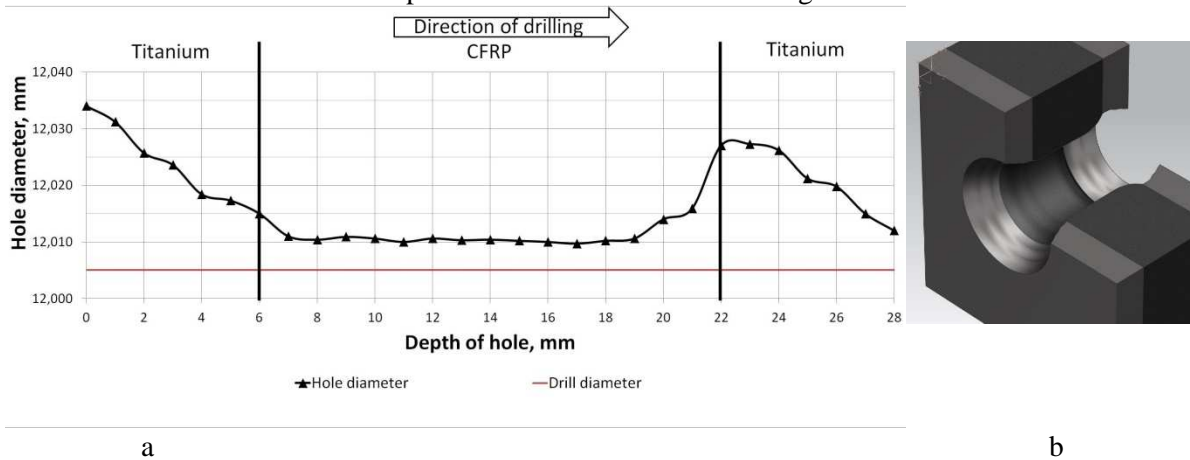


**Figure 4.** Shape of the longitudinal hole section profile (a); hole model (b) ( $s=0.05$  mm/min;  $v=15.08$  m/min;  $l=190$  m)

Figure 4 shows that drilled holes in titanium become cone-shaped due to the described thermal effects. Hole diameters increase at the drill enter point. The holes in CFRP have constant diameters due to steady-state cutting temperatures and insignificant effects of a linear CFRP expansion coefficient. At the end of the drilling of CFRP and at the beginning of the drilling of the second titanium layer, increase in diameter caused by the thermal drill expansion at the beginning of the drilling of titanium occurs.

Regression models for hole shape accuracy and surface roughness were developed taking into account the following factors:  $X_1$  (cutting speed rate  $v$ ),  $X_2$  (feed rates),  $X_3$  (block factor – cutting length  $l$ ). Natural and standard levels of plan factors are presented in Table 1.

**Table 1.** Natural and standard levels of plan factors

Natural levels of factors			Standard levels of factors	
Cutting speed rate, $v$ m/min ( $X_1$ )	Feed rate, $s$ mm/rev ( $X_2$ )	Cutting length (block factor), $l$ m ( $X_3$ )	Key factors $X_1, X_2$	Block factor $X_3$
15.08	0.075	0-243.2	1	1
10.18	0.05	243.2-486.4	0	2
5.28	0.023	486.4-729.6	-1	3

Response surfaces of longitudinal section profile deviation for the whole stack and the first titanium layer are shown in Figure 5.

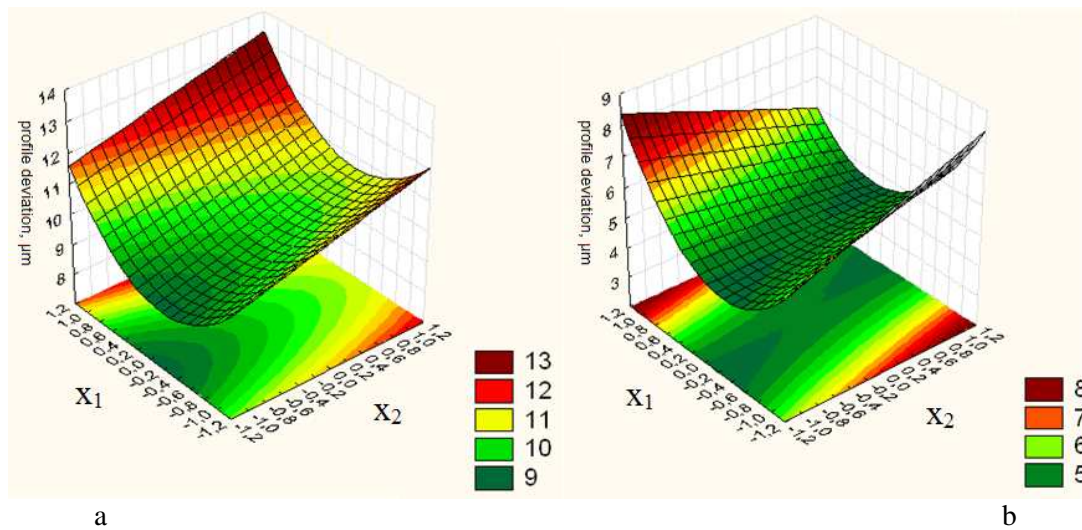


**Figure 5.** Relationship of the longitudinal section profile deviation and cutting modes a) for the whole stack, b) for the first titanium layer.

Figure 5a shows that the maximum deviation  $\Delta$  of the longitudinal section profile corresponds to the maximum cutting speed rate  $v=15.08$  m/min, feed rate  $s=0.075$  mm/rev and cutting length. The minimum deviation corresponds to the minimum feed rate  $s=0.023$  mm/rev and average cutting speed rate  $v=10.18$  m/min. When the feed rate increases, linear function growth occurs. When the cutting rate increases or decreases to the average cutting speed rate  $v=10.18$  m/min, parabolic function growth occurs. Thus, to improve performance with minimum effects on profile deviations, it is necessary to increase the feed rate.

Similar relations of the longitudinal section profile and all the layers  $\Delta_{Ti1}$ ,  $\Delta_{CFRP}$ ,  $\Delta_{Ti2}$  were determined (Figure 5b). The analysis of these surfaces makes it possible to conclude that titanium has the most significant effects on general longitudinal section profile deviations. Variability deviation intervals are such that the first titanium layer forms the upper boundary of the general profile deviation, and the CFRP layer forms the lower boundary of the profile deviation. For the titanium layers, response surface shapes are similar. Maximum response occurs at a maximum feed rate  $s=0.075$  mm/min and a minimum cutting speed rate  $v=5.28$  m/min, and at a maximum speed rate  $v=15.08$  m/min and a minimum feed rate  $s=0.023$  mm/min. The area of minimum response values corresponds to average cutting speed rates. In this case, there are no feed effects in the first layer and minimum feed effects in the second one. The response surface for the longitudinal section profile deviation in the CFRP layer differs from the surface shape in titanium. The maximum value can be observed at the largest feed rate  $s=0.075$  mm/min and cutting speed rate  $v=15.08$  m/min, the minimum value can be observed at a maximum cutting speed rate  $v=15.08$  m/min and a minimum feed rate  $s=0.023$  mm/min. It is in line with existing concepts of CFRP cutting processes (maximum cutting speed rate, minimum feed rate). Block factor X3 (cutting length  $l$ ) does not influence the response shape for all the layers but increases response values.

Corresponding regression models were developed for surface roughness parameters Ra and Rz. Response surfaces for parameters  $Ra_{Ti1}$ ,  $Ra_{CFRP}$  are shown in Figure 6.

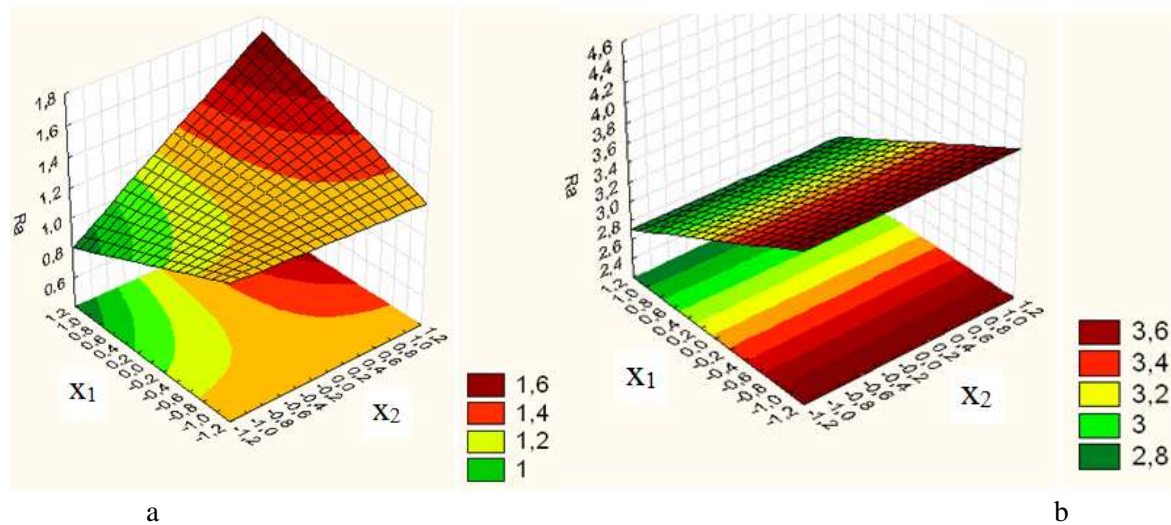


**Figure 6.** Relationship between hole roughness parameters and cutting modes: in first titanium layer RaTi1 (a); in CFRP RaCFRP (b)

The analysis of response surfaces showed that in the first titanium layer, regressors X2 and X1X2 have similar effects on roughness Ra. At low cutting speed rates, their effects are neutralized, while at maximum cutting speed rates, feed effects are pronounced. A low feed rate  $s=0.023$  mm/rev causes the minimum surface roughness, while a high feed rate  $s=0.075$  mm/rev – the maximum one. The cutting length generates linear and quadratic effects. In the second titanium layer, increase in a feed rate has a negative effect on Ra. Cutting speed rates produce less significant effects, but their increase reduces the roughness. The minimum roughness corresponds to the high cutting speed rate  $v=15.08$  m/min and the low feed rate  $s=0.023$  mm/r. The maximum response corresponds to the low cutting speed rate of  $v=5.28$  m/min and high feed rate of  $s=0.075$  mm/rev.

The response surface for Ra in CFRP is different from similar surfaces of titanium layers. There are no feed effects and insignificant cutting speed effects. Increase in the cutting speed rate decreases the roughness as the more dynamic cutting process contributes to clear cutting of CFRP fibers.

Response surfaces for RzCFRP, RzTi2 are shown in Figure 7. The response surface for Rz in the first titanium layer follows the shape of the response surface for Ra in the same layer. The only difference is that there is no dependency on the cutting length. In the second titanium layer, Rz showed both linear and quadratic dependencies on the feed rate. Thus, increase in the feed rate caused faster growth of the function. There was no cutting speed rate effect on Rz. In CFRP, an interesting relationship was identified for Rz. As distinct from Ra, linear and quadratic feed rate effects were observed. Cutting speed rate effects were also negative. Thus, Rz in CFRP takes a minimum value at high cutting speed rates  $v=15.08$  m/min and average feed rates  $s=0.05$  mm/rev. It takes maximum values at low cutting speed rates  $v=5.28$  m/min and at both the low feed rate  $s=0.023$  mm/rev and high feed rate  $s=0.075$  mm/rev.

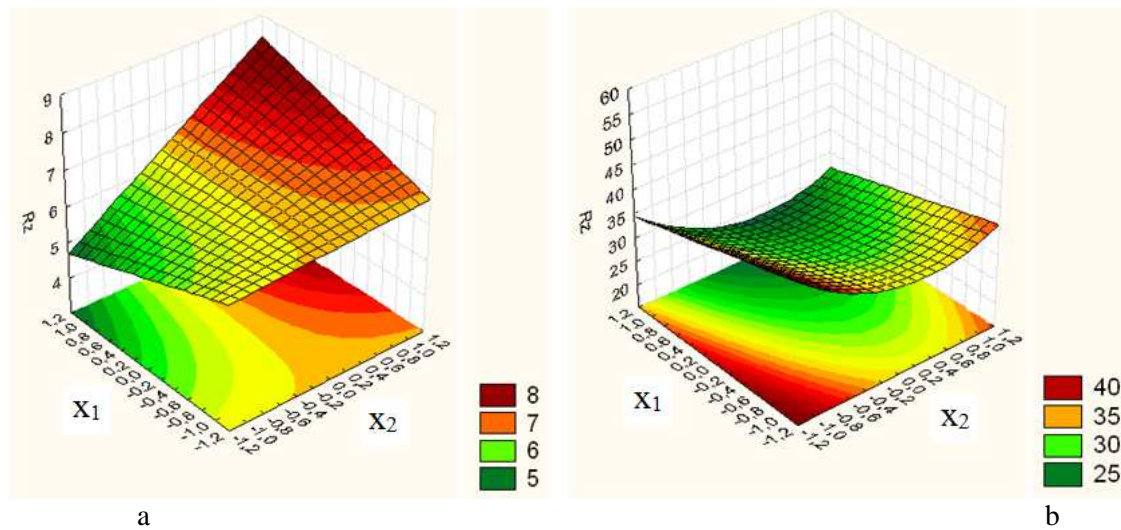


**Figure 7.** Relationship of the hole roughness and cutting modes: in first titanium layer RzTi1 (a); in CFRP RzCFRP 1 (b)

As a part of the experiments (see Figure 3), average temperatures were recorded for cutting modes at  $s=0.05$  mm/min;  $v=15.08$  m/min. When starting the experiment, the cutting length was  $l=710-750$  m.

The average temperature in a cone-shaped surface in titanium was 920C, on the front tool surface – about 3000C. The average temperature of the hole in CFRP was 370C, on the front tool surface – 740C (Figure 8).

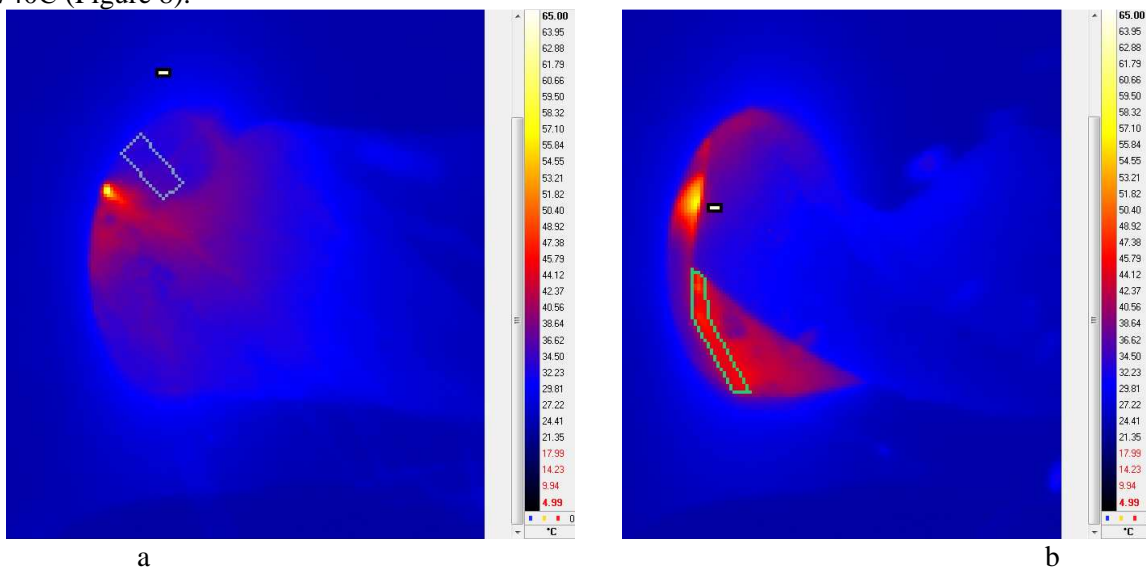


**Figure 8.** Thermographs and temperature recording zones for the material (a) and the tool (b) during the drilling of CFRP

The results got in line with authors' data [28]. The authors used thermocouples for recording temperatures when drilling CFRP/Ti stacks at  $s=0.08$  mm/min,  $v=15$  m/min).

Using formulas (1) and (3) for calculating errors resulted from thermal tool and material expansions, let us find:  $\Delta_{(Ti1 \text{ (input)})} = 9.71 \mu\text{m}$ ;  $\Delta_{(CFRP \text{ (installation)})} = 3 \mu\text{m}$ ;  $\Delta = 3.35 \mu\text{m}$ . As a result of the comparison of the calculated longitudinal hole section profile deviation value of  $\Delta = 3,35 \mu\text{m}$  due to thermal deformations and the value  $\Delta = 10.7 \mu\text{m}$  obtained using contact methods, one can see that the share of thermal deformation effects on the longitudinal section profile deviation is 31%.



As a part of the study of MQL effects on the surface roughness (see Figure 9), it was identified that MQL feed has no effects on the surface roughness in CFRP. In titanium without MQL, the roughness decreases two or more times, i.e. the hole generation in titanium is impossible if there are high roughness requirements.

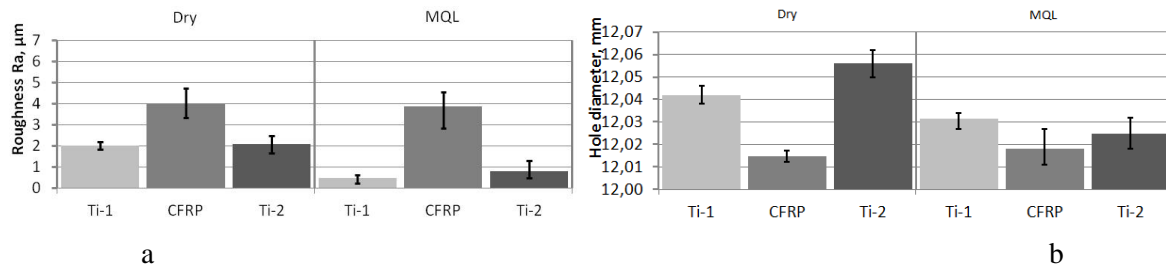


**Figure 9.** Relationship of roughness (a) and diameters (b) holes and MQL use (HAM PRÄZISION 271 Nirodrill,  $v=7.54$  m/min,  $s=0.05$  mm/rev).

The same is true for diametric sizes. MQL has an insignificant effect on a hole diameter in CFRP. In titanium, dry drilling increases variation of hole diameters more than two times. Thus, MQL application for the hole generation in Ti/CFRP stacks contributes to more accurate holes.

## 6. Hole quality and drilling performance optimization

Let us optimize the hole generation in Ti/CFRP stacks using Statistica 6.

Tolerance level N9 for the hole diameter of 10-18 mm is 43  $\mu\text{m}$ . It takes into account the machining tolerance, tool making and tool wear. The working part of drills has a 10  $\mu\text{m}$ -tolerance. A wear tolerance is about 3  $\mu\text{m}$ . Thus, a machining tolerance is 30  $\mu\text{m}$ . The part of the tolerance compensates for hole circularity deviations. As far as we did not manage to identify relations between cutting modes and circularity deviations, let the shape deviation be 1/3 of the remaining tolerance limit ( $30 \cdot 1/3 = 10$   $\mu\text{m}$ ). Thus, the longitudinal section profile deviation should not exceed 10  $\mu\text{m}$ .

Let us find optimal cutting modes based on the cutting speed rate interval of 5.28-15.08 m/min. Machining time for one hole can be calculated by formula [29]:

$$T_M = \frac{(l + l_{rot} + l_{move})\pi d}{1000sv}, \quad (10)$$

where  $l$  – hole depth,  $l_{rot} + l_{move}$  – cutting and overtravel length (for drilling  $\varnothing 12$  mm  $l_{rot} + l_{move} = 5.5$  mm),  $d$  – drilling diameter,  $s$  – feed rate,  $v$  – cutting speed rate.

To find optimal cutting modes, let the desirability function value be equal to 1 for low and average response function values, and 0 - for admissible limit values. To find cutting modes ensuring maximum hole quality, let the desirability function value be equal to 1 for low response function values, 0.5 - for average values, and 0 – for high values. Let us calculate desirability functions for a block factor corresponding to the maximum cutting length. The surfaces of corresponding desirability functions are shown in Figure 10.

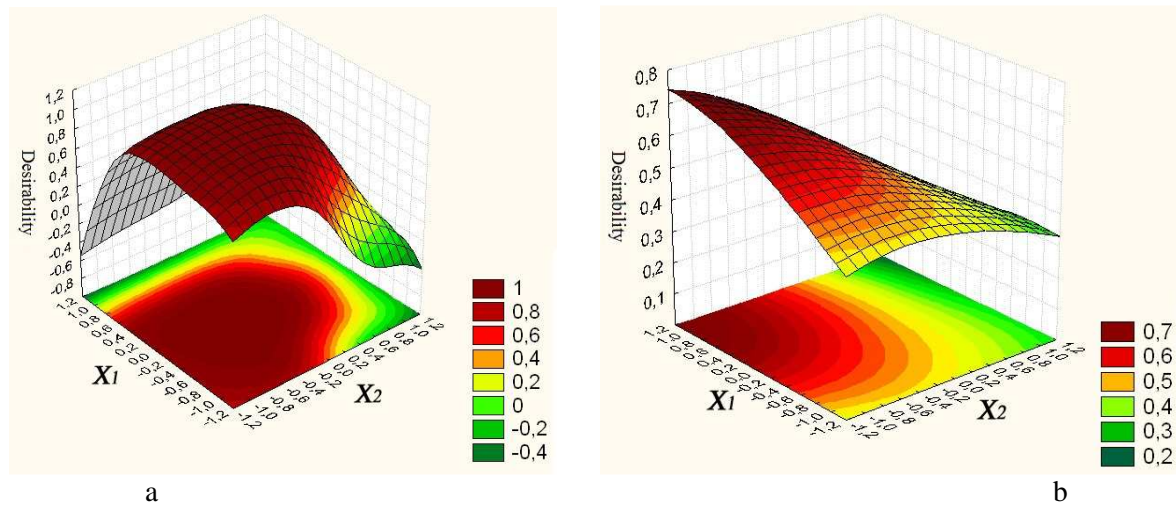


**Figure 10.** Desirability functions for performance (a) and hole quality (b) optimization

Thus, one can conclude that the maximum desirability function corresponds to the cutting modes  $X_2 = 0.4$  ( $s = 0.06$  mm/rev), and  $X_1 = 0.5$  ( $v = 12.63$  m/min). As factors  $X_2$  and  $X_1$  increase, the desirability function sharply decreases which is indicative of an admissible limit response value. That mode corresponds to the maximum performance, machining time is  $T_M = 1.67$  min which is by 2.4 times less than the basic value. The maximum desirability function for hole quality optimization is  $X_2 = -1$  ( $s = 0.023$  mm/rev),  $X_1 = 0.5$  ( $v = 12.63$  m/min). The cutting speed rate does not vary, and the feed rate decreases to minimum values. These changes help to reduce roughness in titanium. Machining time increases by 7%.

The results obtained and equipment and tool recommendations have been used by Irkutsk Aviation Plant – a branch of the JSC Irkut Corporation - for machining holes of MS-21 wing-center section junctures.

## 7. Conclusions

The experiments showed that the best solution for improving accuracy and quality of holes in hybrid stacks is a combination of tools and cutting modes taking into account properties of the materials applied. The following results were obtained:

1. Models of multivariate analysis of variance describing relations between cutting modes and hole accuracy in three-layer hybrid stacks were developed. The models reduce the duration of pre-production and make it possible to specify cutting modes depending on roughness and hole accuracy requirements.

2. Based on the theoretical and experimental studies, the tasks of performance improvement, surface quality and hole accuracy in Ti/CFRP stacks were solved by choosing rational cutting modes. The cutting speed rate of 12.63 m/min, and the feed rate of 0.06 mm/rev are key factors of the optimal cutting mode. It improves performance by 2.4 times.

3. The most important factors influencing hole accuracy parameters, in particular longitudinal hole section profile deviations, are the cutting speed rate and feed rate.

4. Roughness formation models for the first and second titanium layers are different from each other. The dominant factor influencing the roughness is a feed rate. A product of the feed rate and the cutting rate also creates a significant effect with a large regression coefficient.

5. A standard longitudinal section profile shape typical for drilled holes in Ti/CFRP/Ti stacks was identified. A longitudinal section contour in a hybrid stack is as follows: in the titanium layer, a conic shape with an increased diameter at the drill enter point, in CFRP, a constant diameter; in the sections close to the second titanium layer, an increased hole diameter..

6. It was identified that dry drilling decreases accuracy and quality of holes in Titanium 1 two or more times, but the hole roughness in CFRP remains unchangeable.

## References

- [1] Vorobyev Y A, Nikolaenko A I, Vorobyev A Y 2008 Analysis of researches on drilling hybrid CFRP/Ti stacks *Aerospace machines and technologies* **2** 32–38
- [2] Tsao C C 2008 Investigation into the effects of drilling parameters on delamination by various step–core drills *Journal of materials processing technology* **206** 405–411
- [3] Nabhani F 2001 Machining of aerospace titanium alloys *Robotics and Computer–Integrated Manufacturing* **17** (1–2) 99–106
- [4] Shyha I, Soo S, Aspinwall D K, Bradley S, Dawson S, Pretorius S J 2010 Drilling of Titanium/CFRP/Aluminium Stacks *Key Engineering Materials* **447–448** 624–633
- [5] Chigrinets E G 2016 Optimization of drilling of the fiberglass longeron of the rotor blade *Vestnik of MAI* **23** (1) 177–188
- [6] Kuo C –L, Soo S, Aspinwall D, Thomas W, Carr C, Pearson D, M'Saoubi R, Leahy W 2015 Performance of multi–margin coated tools in one–shot drilling of metallic–composite stack materials under varying feed rate and pecking conditions *In Proceedings of the 38th International Matador Conference* (Huwei) 231–238
- [7] Lomaev V I, Dudarev A S 2006 Potential of hole machining during the production of CFRP civil aviation products *Machine building technology* **7** 18–22
- [8] Atarsia A, Mueller–Hummel P, Hollenbaugh S 2013 High efficiency in machining carbon fiber composites and metal stacks for aerospace application *Finer Points* **2013** 18–28
- [9] Seti–Tec website: <http://www.seti–tec.com/>
- [10] Pikalov A A 2012 Peculiarities of hole making in hybrid KM–Ti–Al stacks *Mechanics and machine building* **2012** 669–679
- [11] Yaroslavtsev V M, Nazarov N G 2013 Efficiency assessment for interrupted cutting based on heat release rate variation trends *Electronic journal Science and education* **2013** 35–42
- [12] Rao R V 2011 *Advanced Modeling and Optimization of Manufacturing Processes* (London: Springer)
- [13] Draper N R, Smith G 2007 *Applied regression analysis* (Moscow: Williams)
- [14] Ivanov Y N, Kaverzin E Y, Chapyshev A P 2013 Experimental studies of thermal material expansion effects during the dry drilling of holes in CFRP/Ti stacks *Bulletin of Irkutsk State Technical University* **10** (81)
- [15] Spiridonov A A 1981 *Experiment planning when studying engineering processes* (Moscow: Machine building)
- [16] 2014 *General machine building time standards and cutting modes for standardized operations using universal and multi-purpose CNC-based tools. Part II. Normativy rezhimov rezanija* (Moscow: economics)